IEEE TRANSACTIONS ON

ELECTRON DEVICES

FEBRUARY 1990 VOLUME 37 NUMBER 2 (ISSN 0018-9383)

A PUBLICATION OF THE IEEE ELECTRON DEVICES SOCIETY

LINDA HALL LIBRARY JAN 25 1990

SPECIAL ISSUE ON PHOTOVOLTAIC MATERIALS, DEVICES, AND TECHNOLOGIES

FOREWORD ..... *C. E. Backus, A. M. Barnett, and D. L. Feucht* 329

PAPERS

Characterization of 23-Percent Efficient Silicon Solar Cells ..... *M. A. Green, A. W. Blakers, J. Zhao, A. M. Milne, A. Wang, and X. Dai* 331
Numerical Modeling of Textured Silicon Solar Cells Using PC-1D ..... *P. A. Basore* 337
A New Cell Structure for Very Thin High-Efficiency Silicon Solar Cells ..... *T. Uematsu, M. Ida, K. Hane, S. Kokunai, and T. Saitoh* 344
Simplified Backside-Contact Solar Cells ..... *R. A. Sinton and R. M. Swanson* 348
Excimer Laser Junction Isolation of Crystalline Silicon Solar Cells ..... *R. H. Micheels and P. E. Valdivia* 353
New Interconnection Technology for Enhanced Module Efficiency ..... *W. Schmidt and K.-D. Rasch* 355
An Analytical Solution for the Collection Efficiency of Solar-Cell Emitters With Arbitrary Doping Profile ..... *F. J. Bisschop, L. A. Verhoef, and W. C. Sinke* 358
Studies of Diffused Phosphorus Emitters: Saturation Current, Surface Recombination Velocity, and Quantum Efficiency ..... *R. R. King, R. A. Sinton, and R. M. Swanson* 365
Wide-Bandgap Epitaxial Heterojunction Windows for Silicon Solar Cells ..... *G. A. Landis, J. J. Loferski, R. Beaulieu, P. A. Sekula-Moisé, S. M. Vernon, M. B. Spitzer, and C. J. Keavney* 372
17.8-Percent Efficiency Polycrystalline Silicon Solar Cells ..... *S. Narayanan, S. R. Wenham, and M. A. Green* 382
A New Spin Cast Process for Mass Production of Polycrystalline Silicon Sheets ..... *I. Hide, T. Matsuyama, M. Suzuki, H. Yamashita, T. Suzuki, T. Moritani, and Y. Maeda* 385
a-$Si_{1-x}C_x$:H Alloys for Multijunction Solar Cells ..... *A. Catalano, J. Newton, and A. Rothwarf* 391
Quality Improvement in a-Si Films and Their Application to a-Si Solar Cells ..... *T. Matsuoka and Y. Kuwano* 397
Numerical Modeling of an Amorphous-Silicon-Based p-i-n Solar Cell ..... *A. H. Pawlikiewicz and S. Guha* 403
$CuInSe_2$ Cells and Modules ..... *K. W. Mitchell, C. Eberspacher, J. H. Ermer, K. L. Pauls, and D. N. Pier* 410
Deposition of $CuInSe_2$ Films by a Two-Stage Process Utilizing E-Beam Evaporation ..... *B. M. Basol and V. K. Kapur* 418
Interpretation of Thin-Film Polycrystalline Solar Cell Capacitance ..... *P. H. Mauk, H. Tavakolian, and J. R. Sites* 422
Structure and Properties of High Efficiency ZnO/CdZnS/$CuInGaSe_2$ Solar Cells ..... *W. E. Devaney, W. S. Chen, J. M. Stewart, and R. A. Mickelsen* 428
Efficient CdTe/CdS Solar Cells and Modules by Spray Processing ..... *S. P. Albright, B. Ackerman, and J. F. Jordan* 434
Lightweight Tandem GaAs/$CuInSe_2$ Solar Cells ..... *B. J. Stanbery, B. D. King, R. M. Burgess, R. W. McClelland, N. P. Kim, R. P. Gale, and R. A. Mickelsen* 438

(*Contents Continued on Back Cover*)

HANWHA 1021

Studies of Diffused Phosphorus Emitters: Saturation Current, Surface Recombination Velocity, and Quantum Efficiency

R. R. KING, STUDENT MEMBER, IEEE, R. A. SINTON, MEMBER, IEEE, AND R. M. SWANSON, MEMBER, IEEE

Abstract—**The surface recombination velocity s for silicon surfaces passivated with thermal oxide, is experimentally determined as a function of surface phosphorus concentration for a variety of oxidation, anneal, and surface conditions. This was accomplished by measuring the emitter saturation current density J_0 of transparent diffusions for which the J_0 is strongly dependent on s. At the lowest doping levels, the value of s was confirmed by measurements of s on substrates with uniform phosphorus doping. The impact of these measurements on solar cell design is discussed.**

I. Introduction

PASSIVATED emitters are an important part of many high-efficiency solar cell designs [1]–[5]. An emitter at a semiconductor surface is said to be passivated if the surface has been treated in such a way as to reduce carrier recombination in the emitter. Such emitters can have an emitter saturation current density J_0 that is an order of magnitude lower than that of an unpassivated emitter [3], [6]. Moreover, the minimum J_0 of passivated emitters occurs for shallow, relatively lightly doped diffusions, so the quantum efficiency of this type of emitter located on the sunward surface of a solar cell can be very high while maintaining low J_0. In contrast, the J_0 of unpassivated emitters decreases with increasing emitter thickness and surface dopant concentration [6], [7], which compromises quantum efficiency. An oxide-passivated emitter in silicon also has some advantages over an oxidized silicon surface with the same doping density as the substrate. For solar cells with a substrate in high-level injection, at low incident light intensities, recombination in a passivated emitter at the surface can be much lower than at an oxidized, undoped surface [4], [8]. In addition, the recombination characteristics of passivated emitters have been found to be much more resistant to degradation by UV light than those of an oxidized, undoped surface [9].

One of the most important parameters for predicting the J_0 and the quantum efficiency of a passivated emitter is the surface recombination velocity s as a function of surface dopant concentration N_{surf}. Unfortunately, s is strongly dependent on technological factors, some of which are difficult to control. For an oxidized silicon surface, s varies with surface roughness, surface contamination, oxidation temperature, ambient gases during oxidation, and postoxidation annealing. When contamination is negligible and all processing parameters are the same, however, definite trends in the dependence of s on N_{surf} can be observed.

This paper reports experimental measurements of the emitter saturation current density for a variety of emitters, with differing surface concentration and junction depth. Values of surface recombination velocity extracted from this data are presented along with calculations of emitter saturation current density and photocurrent loss based on this new information.

II. Previous Work

Many workers have studied recombination at the oxidized silicon surface. Some of their contributions include: measurement of increasing density of interface states N_{it}, with increasing phosphorus, arsenic, boron, or gallium concentration in the silicon, and higher fixed oxide charge for boron doping than for phosphorus doping [10]; deep level transient spectroscopy measurements of the interface state density per unit energy D_{it}, and of electron and hole capture cross sections σ_n and σ_p on nearly intrinsic silicon [11]; the decrease in the measured J_0 of oxide passivated boron emitters with increasing oxidation temperature [1]; measurements of the J_0 of oxide-passivated phosphorus and boron diffusions by contactless photoconductivity decay [6]; the σ_n/σ_p ratio of the interface traps that dominate recombination for lightly boron-doped, oxidized surfaces [12]; and measurement of the decrease in s at a lightly boron-doped Si/SiO_2 interface with increasing injected carrier density [13], [14].

Finally, several authors have measured the fundamental surface recombination velocity s_0 at oxidized, boron-doped silicon surfaces [15]–[17]. In principle, s_0 can be used to predict the actual surface recombination velocity s, but, in practice, the predicted value of s is a very sensitive function of the surface potential and of the ratio σ_n/σ_p. This leads to a large uncertainty in the value of s when calculated in this way. In addition, using s_0 as a parameter to characterize recombination at the Si/SiO_2 interface requires the assumption that D_{it}, σ_n, and σ_p are

Manuscript received April 30, 1989; revised October 2, 1989. This work was supported by the Department of Energy through Sandia National Laboratories.

The authors are with Stanford University, Stanford, CA 94305.

IEEE Log Number 8932891.

0018-9383/90/0200-0365$01.00 © 1990 IEEE

constant with respect to bandgap energy. These approximations become less valid as the Fermi-level splitting becomes large, as in a passivated solar cell emitter.

III. Experimental Method Used in this Work

Contactless photoconductivity decay [6], [18] was used to measure surface and bulk recombination in this study. In this method, the sample to be measured is placed on a coil with an oscillating magnetic field. The coil couples inductively to the sample, and the measured signal output of the circuit containing the coil is proportional to the conductance of the sample. A pulse of light from a strobe lamp generates carriers in the silicon sample. After several transit times of the wafer have elapsed, the excess carrier concentration n' has a nearly uniform distribution throughout the wafer. The decay of n' is then recorded as a function of time. The effective lifetime τ_{eff} of the sample as a whole is given by:

$$\frac{1}{\tau_{\text{eff}}} \equiv -\frac{1}{n'}\frac{dn'}{dt}.$$

Both surface and bulk recombination components are included in τ_{eff}. Most of the samples consisted of a lightly doped silicon substrate that has identical planar dopant diffusions with thermal oxide passivation on both sides of the wafer. The substrate was in high-level injection during the measurement of τ_{eff}. The doped surfaces are in low-level injection. Since the substrate is highly injected, n' is almost exactly equal to n, the total electron concentration, and τ_{eff} depends on n according to the expression:

$$\frac{1}{\tau_{\text{eff}}} = \frac{1}{\tau_{\text{bulk}}} + 2J_0\frac{n}{qn_i^2 w} + C_A n^2$$

where τ_{bulk} is the bulk Schockley–Read–Hall (SRH) lifetime, J_0 is the emitter saturation current density of a single dopant diffusion, w is the wafer thickness, and C_A is the ambipolar bulk Auger coefficient [6]. When $(1/\tau_{\text{eff}}) - C_A n^2$ is plotted versus n, a straight line results which has a slope proportional to J_0. Thus this method yields a fairly direct measurement of J_0. The value of C_A used for the highly injected substrate was 1.66×10^{-30} cm^6/s from [19], and was assumed to have an uncertainty of ± 10 percent. After the lifetime measurements, the oxide was stripped from the samples, the sheet resistance of each diffusion was measured, and the dopant profile was measured by secondary ion mass spectroscopy (SIMS).

In the low doping range, τ_{eff} was also measured for some uniformly doped substrates with oxidized surfaces. In this case, τ_{eff} is given by:

$$\frac{1}{\tau_{\text{eff}}} = \frac{1}{\tau_{\text{bulk}}} + \frac{2}{w}s$$

where s is the surface recombination velocity. When several samples with identical doping and processing but different thicknesses are measured, $1/\tau_{\text{eff}}$ can be plotted versus $2/w$ to give a straight line with slope s and a $(1/\tau_{\text{eff}})$-axis intercept of $1/\tau_{\text{bulk}}$.

IV. Experimental Data

Fig. 1 shows some of the measured values of J_0 at 300 K for oxide-passivated phosphorus diffusions, and how they depend on $N_{D,\text{surf}}$, the surface phosphorus concentration, and x_j, the emitter thickness at which $N_D = 10^{16}$ cm^{-3}. The samples shown were processed in slightly different ways. Some were oxidized in an ambient containing trichloroethane (TCA). Some were not. Some were given a forming gas anneal (FGA) at 400°C, others were given an aluminum anneal, in which both sides of the wafers were covered with sputtered aluminum, and annealed at 400°C. For all samples, the dopant source was phosphorus doped SiO_2, formed by atmospheric pressure chemical vapor deposition at 400°C.

From Fig. 1, it can be seen that increasing emitter thickness or increasing $N_{D,\text{surf}}$ tends to increase the J_0, as bulk recombination in the emitter dominates over surface recombination. J_0 is lowest for shallow, lightly doped emitters. The J_0 remains small even for emitters with very low $N_{D,\text{surf}}$, in spite of the lower potential barrier between the surface and the bulk of the wafer that exists for such emitters. This is because s decreases with decreasing $N_{D,\text{surf}}$, which tends to counteract the detrimental effect of the lower potential barrier.

Fig. 2 is a similar plot showing the experimental J_0 dependence on $N_{D,\text{surf}}$, for passivated emitters that have not received a forming gas anneal. The forming gas anneal makes little difference at high doping concentrations, presumably because hydrogen cannot passivate the traps that are most active in causing recombination. Below $N_{D,\text{surf}} = 6 \times 10^{18}$ cm^{-3}, however, the higher s of the samples without an FGA begins to impact the J_0 seriously.

Since most high-efficiency silicon solar cells have a textured sunward surface, it is important to know what effect texturing has on the J_0. Fig. 3 shows measured values of J_0 for passivated emitters with a textured surface. $N_{D,\text{surf}}$ and x_j could not be measured directly on the textured samples by SIMS, because of the rugged topography of the surface. Instead, the values of $N_{D,\text{surf}}$ and x_j used in Fig. 3 are those measured on companion wafers that were processed identically, except that they were untextured. The value of J_0 for the textured emitters is typically higher than for the corresponding untextured emitter, but the same trends of lower J_0 with decreasing $N_{D,\text{surf}}$ and decreasing x_j persist in the textured case.

V. Dependence of Surface Recombination Velocity on Phosphorus Concentration

A. Extraction of Surface Recombination Velocity from J_0

Since the dependence of J_0 on $N_{D,\text{surf}}$ in the phosphorus emitters is determined at least in part by the dependence of s on $N_{D,\text{surf}}$, it is possible to extract information about s as a function of $N_{D,\text{surf}}$ from J_0 measurements. This was done by solving the carrier transport equations numerically, in the manner described by del Alamo [7]. To extract s in this way requires well-known values of the prop-

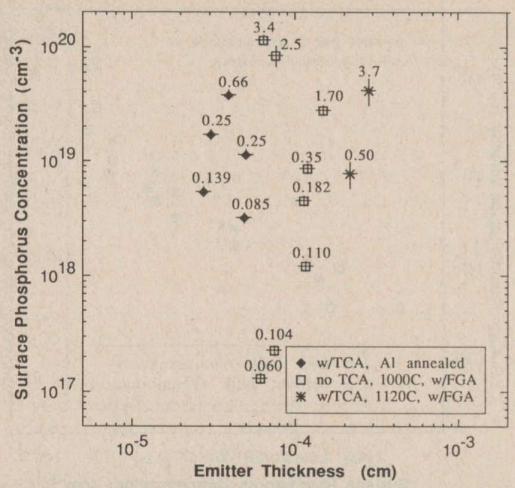

Fig. 1. Measured values of the emitter saturation current density J_0 for untextured, oxide-passivated phosphorus diffusions, after either a forming gas anneal or an aluminum anneal. The values of surface phosphorus concentration $N_{D,\text{surf}}$ and emitter thickness at $N_D = 10^{16}$ cm^{-3}, x_j, were measured by SIMS. The value of J_0, in units of 10^{-13} A/cm^2, is printed above each point.

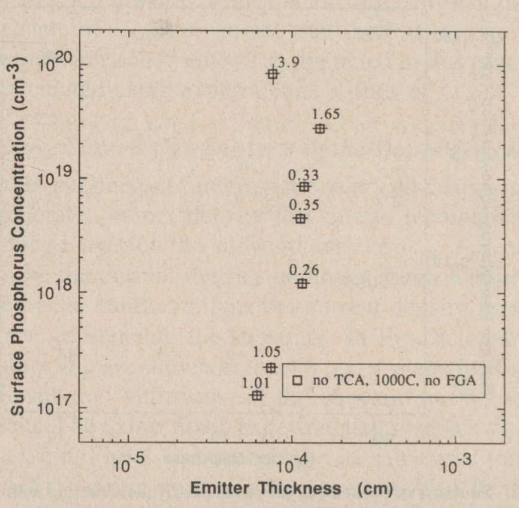

Fig. 2. Measured values of the emitter saturation current density J_0 for untextured, oxide-passivated phosphorus diffusions, with no forming gas anneal. The values of surface phosphorus concentration $N_{D,\text{surf}}$ and emitter thickness at $N_D = 10^{16}$ cm^{-3}, x_j, were measured by SIMS. The value of J_0, in units of 10^{-13} A/cm^2, is printed above each point.

erties that control carrier transport, such as minority carrier lifetime, minority carrier mobility, and bandgap narrowing, all as a function of N_D. Fortunately, these parameters are known with a high degree of confidence from previous experiments [7], with the possible exception of lifetime for doping lower than $N_D \approx 5 \times 10^{17}$ cm^{-3}. Above $N_D \approx 10^{18}$ cm^{-3}, hole lifetime in the heavily phosphorus doped emitter should be dominated by band-to-band Auger recombination. Since this process is fundamental, in that it does not depend on defect density in the silicon, the value of the Auger coefficient found in previous experiments should be quite applicable to the emitters in this study. In addition, the contribution of bulk recombination in the emitter to the measured J_0 can be minimized by using very thin emitters, improving the accuracy of s. The experimental uncertainty in bandgap narrowing is ± 9 meV out of 81 meV at $N_D = 5.3 \times 10^{19}$ cm^{-3} [7].

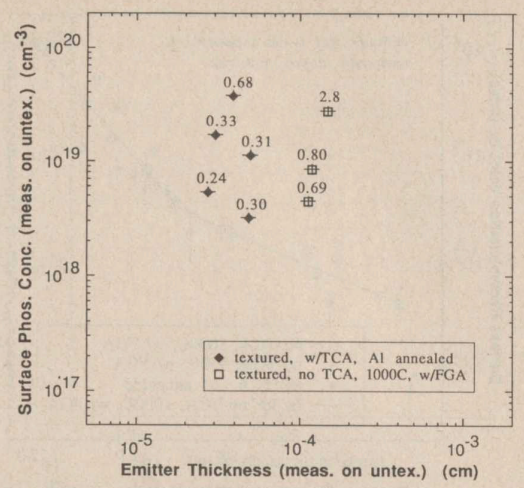

Fig. 3. Measured values of the emitter saturation current density J_0 for textured, oxide-passivated phosphorus diffusions, after either a forming gas anneal or an aluminum anneal. The values of surface phosphorus concentration $N_{D,\text{surf}}$ and emitter thickness at $N_D = 10^{16}$ cm^{-3}, x_j, were measured by SIMS on untextured wafers that were otherwise processed identically to the textured wafers. The value of J_0, in units of 10^{-13} A/cm^2, is printed above each point.

B. Surface Recombination Velocity Versus Phosphorus Concentration

Given the SIMS measurements of phosphorus concentration as a function of depth and the measured values of J_0, the numerical emitter model was used to find s for each emitter. The results are shown in Fig. 4. Most of the emitters used to find s were thin enough that the J_0 was dominated by surface recombination rather than bulk recombination, to make the measurement as sensitive to s as possible. The extracted values of s show a remarkable correlation with $N_{D,\text{surf}}$, especially for a parameter that is as process dependent as s. Note that the aluminum annealed samples have a consistently lower s than those that received an FGA. Also, a 950°C oxidation seems to yield a somewhat higher s than one at 1000°C.

For $N_{D,\text{surf}}$ greater than about 10^{18} cm^{-3}, the increase in s is approximately linear in $N_{D,\text{surf}}$. This is the behavior one would expect if the increased s were due solely to an increase in interface states with a constant capture cross section, and if the interface state density were proportional to the surface density of phosphorus atoms. This is an over-simplified explanation, since the cross section probably does depend on bandgap energy and the surface recombination rate is dependent on the quasi-Fermi-level positions at the surface.

The points indicated by stars in Fig. 4 were measured on samples with uniform phosphorus doping throughout the wafer, using several different wafer thicknesses. This measurement does not require any assumption of the dependence of bulk lifetime on N_D, and serves as a check on the values of s extracted from emitter measurements.

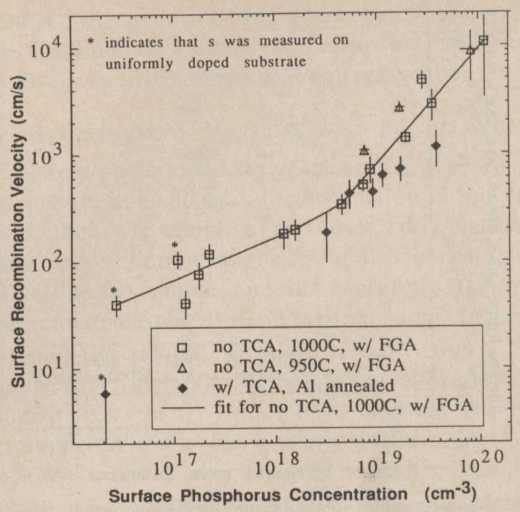

Fig. 4. Surface recombination velocity s extracted from measurements of J_0 on untextured, oxide-passivated phosphorus diffusions, using a numerical emitter model. The value of s for the starred points was measured using several thicknesses of wafers with uniform phosphorus doping.

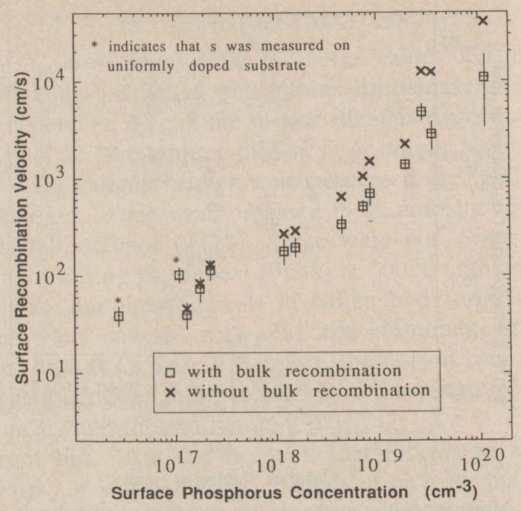

Fig. 5. Surface recombination velocity s extracted for both the standard case, in which the bulk recombination in the passivated emitter is accounted for, and the case in which there is no bulk recombination. The latter case gives an upper limit for s.

It was found that the value of s is dependent on injection level in the uniformly doped substrate: s decreases with increasing excess carrier concentration. Evidence for this phenomenon was also observed for the three emitters with $N_{D,\text{surf}} < 3 \times 10^{17}$ cm^{-3}. The $(1/\tau_{\text{eff}}) - C_A n^2$ versus n curves for these emitters were not straight lines as they were for all the other emitters in this study. Instead, they curve down as n increases, indicating that the recombination rate is lower than expected at high values of n. This could be explained by an injection-level-dependent value of s that decreases as n increases. The J_0 values for these three samples were taken in the limit of low n, where the $(1/\tau_{\text{eff}}) - C_A n^2$ versus n curves become nearly linear. The values of s found for the uniformly doped substrates were measured at $n = 3.0 \times 10^{15}$ cm^{-3}.

To show how small the contribution of bulk recombination in the emitter to the total J_0 is in these transparent emitters, the value of s extracted in the absence of bulk recombination is plotted in Fig. 5. In this case, all recombination is attributed to surface recombination, so these values of s are an upper limit given the bandgap narrowing and mobility measured by del Alamo, and the measured values of J_0. Comparison of the points calculated with and without bulk recombination shows that more than half of the recombination in the emitter takes place at the surface for most of the emitters.

VI. Discussion

A. Emitter Saturation Current Density

The experimentally determined dependence of s on $N_{D,\text{surf}}$ from the last section can be combined with the lifetime, mobility, and bandgap narrowing data in [7] to generate a contour plot of J_0 for oxide-passivated phosphorus diffusions, as a function of both $N_{D,\text{surf}}$ and x_j. This has been done in Fig. 6, for diffusions with a Gaussian phosphorus concentration profile. The s versus $N_{D,\text{surf}}$ data used

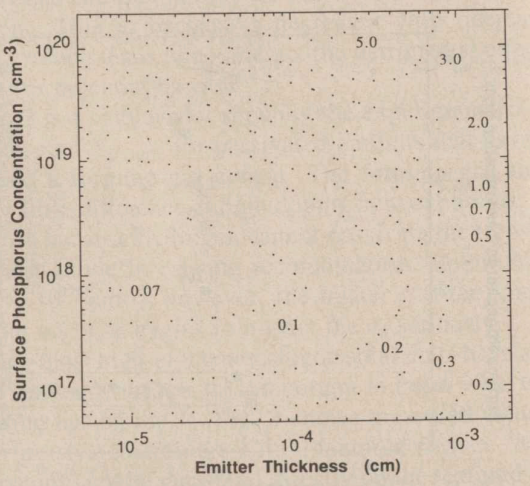

Fig. 6. Contours of constant J_0 for oxide-passivated emitters with a Gaussian phosphorus profile. The dependence of s versus $N_{D,\text{surf}}$ used is the fit shown in Fig. 4, which was experimentally determined for emitters with an untextured surface, oxidized at 1000°C with no TCA, and with an FGA. The contours are labeled with the corresponding value of J_0, in units of 10^{-13} A/cm^2.

was for samples with a 1000°C oxidation, no TCA during oxidation, that received an FGA. The value of s was found for a given $N_{D,\text{surf}}$ from the fit shown in Fig. 4. Since this contour plot was generated from J_0 data such as that shown in Fig. 1, it naturally agrees with that data. Because this contour plot is based on experimental s values, it should be more useful for predicting the J_0 of oxide-passivated diffusions than emitter modeling based on an assumed value of s. In the previous absence of data on s as a function of $N_{D,\text{surf}}$, a common practice was to use a constant value of s, e.g., 1000 cm/s, to predict the J_0 of passivated emitters. Fig. 7 is a contour plot of J_0 that assumes $s = 1000$ cm/s. A comparison between Figs. 6 and 7 indicates that the inclusion of the doping dependence of s fundamentally changes the trends in J_0. Most notably, for

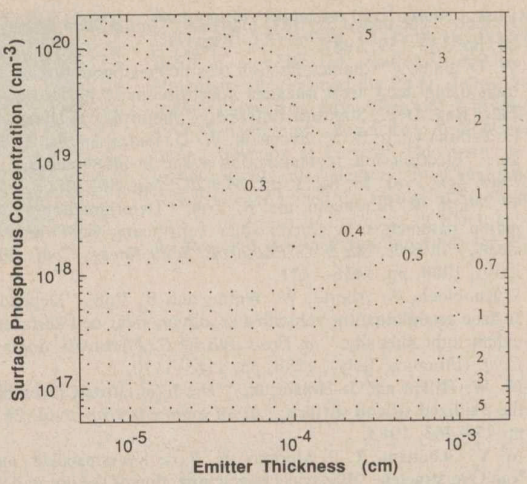

Fig. 7. Contours of constant J_0 for oxide-passivated emitters with a Gaussian phosphorus profile assuming $s = 1000$ cm/s. The contours are labeled with the corresponding value of J_0, in units of 10^{-13} A/cm^2.

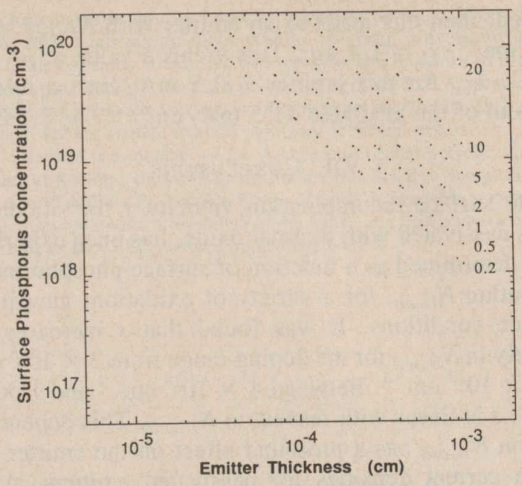

Fig. 8. Contours of constant J_{lost} for oxide-passivated emitters with a Gaussian phosphorus profile. J_{lost} is the photogenerated current density that is lost due to recombination in the emitter. The dependence of s versus $N_{D,\text{surf}}$ used is the fit shown in Fig. 4, which was experimentally determined for emitters with an untextured surface, oxidized at 1000°C with no TCA, and with an FGA. J_{lost} was calculated for the SERI AM1.5 direct normal solar spectrum incident on the cell, normalized to have an incident intensity of 0.100 W/cm^2 (one sun). The photogenerated current density in 0.1 cm of silicon is 0.0415 A/cm^2 for this spectrum. The contours are labeled with the corresponding value of J_{lost}, in units of 10^{-3} A/cm^2.

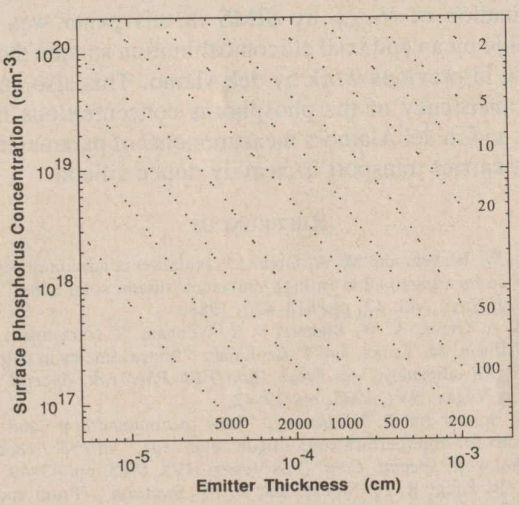

Fig. 9. Contours of constant $\rho_\square$ for emitters with a Gaussian phosphorus profile, using the majority carrier mobility data of Thurber. The contours are labeled with the corresponding value of $\rho_\square$, in $\Omega/\square$.

the doping range less than 10^{18} cm^{-3}, the use of an $s = 1000$ cm/s assumption leads to an order-of-magnitude overestimate of J_0. One can see that there is a large discrepancy between the value of J_0 predicted in this plot and those calculated using experimental values of s.

B. Photogenerated Current Loss in the Doped Layer

Another parameter of interest for solar cell design is the photogenerated curent density lost due to recombination in the doped layer on the sunward surface J_{lost}. J_{lost} is defined to be the current density photogenerated within the volume of the emitter, minus the current density flowing out of the emitter into the substrate. In Fig. 8, contours of constant J_{lost} are shown in the $N_{D,\text{surf}}$, x_j plane for Gaussian phosphorus diffusions on the sunward surface of a solar cell. The same fit of experimental s versus $N_{D,\text{surf}}$ data shown in Fig. 4 was used. J_{lost} was calculated for the SERI AM1.5 direct normal solar spectrum [20] incident on the cell, normalized to have an incident intensity of 0.100 W/cm^2 (one sun), and for unity optical transmittance of the sunward surface. For reference, the photogenerated current density in 0.1 cm of silicon is 0.0415 A/cm^2 for this spectrum, using the absorption coefficient data in [21]. J_{lost} is actually quite independent of s, except for deep emitters with low surface concentration.

Fig. 9 gives contours of constant sheet resistance $\rho_\square$ of Gaussian phosphorus diffusions on the same axes as the two previous plots, so that J_0 and J_{lost} may be correlated with $\rho_\square$. The $\rho_\square$ contours were calculated using the majority carrier mobility data from [22]. Comparing Figs. 8 and 9, it is evident that J_{lost} depends mainly on $\rho_\square$ (as the curves are roughly parallel), but that *deeper* emitters (when passivated) tend to have less photocurrent loss than shallower ones of the same sheet resistance.

Two solar cell design cases may illustrate how these plots can be put to use. In the case of a back-contacted cell in which the sunside diffusion is used mainly to reduce surface recombination, not to collect current, the optimum emitter is the one with the lowest J_0. For untextured surfaces, this corresponds an emitter with $N_{D,\text{surf}} \approx 1 \times 10^{18}$ cm^{-3} that is as thin as possible. Fig. 3 shows an emitter with these specifications is probably near optimum in J_0 when it has a textured front surface, as well. Other considerations such as resistance to ultraviolet-induced degradation may play a dominant role in selecting the best emitter of this type [9].

The second case is that of the emitter on the sunward surface of a conventional solar cell contacted on both sides. From Figs. 7–9, one can see that if a value of $N_{D,\text{surf}} > 2 \times 10^{19}$ cm^{-3} is required for low contact resistance, a J_0 of 1×10^{-13} cm^{-3} is desired, and $\rho_\square$ should be max-

imized, then this leads to an emitter with $N_{D,\text{surf}} = 2 \times 10^{19}$ cm^{-3}, $x_j = 1.4$ μm. This yields a value of $\rho_\square = 60$ $\Omega/\square$. J_{lost} for this emitter is 0.5 mA/cm^2, a tolerable loss out of the available 41.5 mA/cm^2.

VII. Conclusions

The surface recombination velocity s for silicon surfaces passivated with thermal oxide, has been experimentally determined as a function of surface phosphorus concentration $N_{D,\text{surf}}$ for a variety of oxidation, anneal, and surface conditions. It was found that s increases sublinearly in $N_{D,\text{surf}}$ for the doping range from 2×10^{15} cm^{-3} to 1×10^{18} cm^{-3}. Between 4×10^{18} cm^{-3} and 1×10^{20} cm^{-3}, s is linear with respect to $N_{D,\text{surf}}$. This dependence of s on $N_{D,\text{surf}}$ has a profound effect on the emitter saturation current densities for passivated emitters. Armed with this new data, it should be possible to make more informed choices in the design of solar cells and other silicon devices.

Acknowledgment

The authors would like to thank A. Cuevas, D. Kane, S. Swirhun, J. del Alamo, P. Gruenbaum, and J.-Y. Gan for many helpful dicussions. J. del Alamo wrote part of the program used for emitter modeling. The accurate determination of $N_{D,\text{surf}}$ by SIMS in this paper was made possible by an epitaxial silicon calibration sample that was grown in previous work by del Alamo. This also ensured the consistency of the phosphorus concentrations in this work and in del Alamo's measurements of parameters that affect carrier transport in heavily doped silicon.

References

[1] A. W. Blakers and M. A. Green, "Oxidation condition dependence of surface passivation in high efficiency silicon solar cells," *Appl. Phys. Lett.*, vol. 47, pp. 818–820, 1985.

[2] M. A. Green, A. W. Blakers, S. R. Wenham, S. Narayanan, M. R. Willison, M. Taouk, and T. Szpitalak, "Improvements in silicon solar cell efficiency," in *Proc. 18th IEEE Photovolt. Special. Conf.* (Las Vegas, NV), 1985, pp. 39–42.

[3] M. Spitzer and C. J. Keavney, "Low recombination p^+ and n^+ regions for high performance silicon solar cells," in *Proc. 18th IEEE Photovolt. Special. Conf.* (Las Vegas, NV), 1985, pp. 43–49.

[4] R. R. King, R. A. Sinton, and R. M. Swanson, "Front and back surface fields for point-contact solar cells," in *Proc. 20th IEEE Photovolt. Special. Conf.* (Las Vegas, NV), 1988.

[5] R. A. Sinton, R. R. King, and R. M. Swanson, "Novel implementations of backside-contact silicon solar cell designs in one-sun and concentrator applications," in *Proc. 4th IREE Photovolt. Sci. Eng. Conf.* (Sydney, Australia), 1989.

[6] D. E. Kane and R. M. Swanson, "Measurement of the emitter saturation current by a contactless photoconductivity decay method," in *Proc. 18th IEEE Photovolt. Special. Conf.* (Las Vegas, NV), 1985, pp. 578–583.

[7] J. A. del Alamo, "Minority carrier transport in heavily doped n-type silicon," Ph.D. dissertation, Elec. Eng. Dep., Stanford University, Stanford, CA, Nov. 1985.

[8] R. R. King, R. A. Sinton, and R. M. Swanson, "Doped surfaces in one-sun, point-contact solar cells," *Appl. Phys. Lett.*, vol. 54, no. 15, pp. 1460–1462, Apr. 10, 1989.

[9] P. E. Gruenbaum, R. A. Sinton, and R. M. Swanson, "Stability problems in point-contact solar cells," in *Proc. 20th IEEE Photovolt. Special. Conf.* (Las Vegas, NV), 1988.

[10] J. Snel, "The doped Si/SiO_2 interface," *Solid-State Electron.*, vol. 24, pp. 135–139, 1981.

[11] W. D. Eades, "Characterization of silicon–silicon dioxide interface traps using deep level transient spectroscopy," Ph.D. dissertation, Elec. Eng. Dep., Stanford University, Stanford, CA, June 1985.

[12] E. Yablonovitch, R. M. Swanson, W. D. Eades, and B. R. Weinberger, "Electron-hole recombination at the Si-SiO_2 interface," *Appl. Phys. Lett.*, vol. 48, no. 3, pp. 245–247, Jan. 20, 1986.

[13] W. Warta, R. Bergmann, and B. Voß, "Determination of recombination parameters in silicon solar cells using light induced transients," in *Proc. 8th E. C. Photovolt. Solar Energy Conf.* (Florence, Italy), 1988, pp. 1416–1421.

[14] J. Knobloch, A. Aberle, W. Warta, and B. Voß, "Dependence of surface recombination velocities at silicon solar cell surfaces on incident light intensity," in *Proc. 8th E. C. Photovolt. Solar Energy Conf.* (Florence, Italy), 1988, pp. 1165–1170.

[15] M. W. Hillen and J. Holsbrink, "The base current recombining at the oxidized silicon surface," *Solid-State Electron.*, vol. 26, no. 5, pp.453–463, 1983.

[16] M. Y. Ghannam, R. P. Mertens, R. F. de Keersmaecker, and R. J. Van Overstraeten, "Electrical characterization of the boron-doped Si–SiO_2 interface," *IEEE Trans. Electron Devices*, vol. ED-32, no. 7, pp. 1264–1271, July 1985.

[17] S. E. Swirhun, "Characterization of majority and minority carrier transport in heavily doped silicon," Ph.D. dissertation, Elec. Eng. Dep., Stanford University, Stanford, CA, June 1987.

[18] H. W. Curtis and R. L. Verkuil, "Lifetime factors in silicon," ASTM, Philadelphia, PA, Special Tech. Pub. 712; also presented at the American Soc. Testing and Materials Symp., San Diego, CA, Feb. 15–16, 1979.

[19] R. A. Sinton and R. M. Swanson, "Recombination in highly injected silicon," *IEEE Trans. Electron Devices*, vol. ED-34, no. 6, pp. 1380–1389, June 1987.

[20] R. J. Matson, Keith A. Emery, and Richard E. Bird, "Terrestrial solar spectra, solar simulation, and solar cell short-circuit current calibration: A review," *Solar Cells*, vol. 11, pp. 105–145, 1984.

[21] M. A. Green, *High Efficiency Silicon Solar Cells.* Brookfield, VT: Trans Tech Publications, 1987, Appendix C.

[22] W. R. Thurber, R. L. Mattis, Y. M. Liu, and J. J. Filliben, "Resistivity-dopant density relationship for phosphorus doped silicon," *J. Electrochem. Soc.*, vol. 127, no. 8, pp. 1807–1812, Aug. 1980.

*

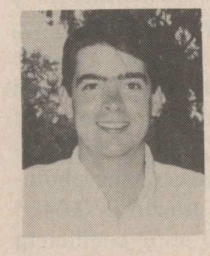

R. R. King (S'87) was born in Chapel Hill, NC, in 1960. He received the B.S. degree in physics and the M.S. degree in electrical engineering from Stanford University, Stanford, CA, in 1985 and 1987, respectively. He is currently working toward the Ph.D. degree in electrical engineering at Stanford University. His research topics include high-efficiency crystalline-silicon solar cells and minority-carrier recombination at the doped Si/SiO_2 interface.

Ronald A. Sinton (S'84–M'87), was born in Denver, CO, in 1959. He received the B.S. degree in engineering physics from the University of Colorado, Boulder, in 1981, and the M.S. and Ph.D. degrees in applied physics from Stanford University in 1984 and 1987, respectively. His dissertation research involved the optimization of silicon solar cells for use in highly concentrated sunlight.

He is now a Research Associate at Stanford University. His primary interest is experimental work in solar photovoltaic devices, a topic about which he has written 25 published articles.

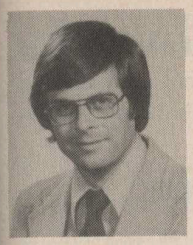

Richard M. Swanson (S'67–M'78), was born in Davenport, IA, on May 13, 1945. He received the B.S.E.E. and M.S.E.E. degrees from Ohio State University in 1969 and the Ph.D. degree in electrical engineering from Stanford University in 1974. Subsequently, he received an IBM postdoctoral fellowship at Stanford University to study techniques for solar-electric power generation.

In 1976 he joined the faculty at Stanford University as Assistant Professor of Electrical Engineering and obtained funding from the Electric Power Research Institute to research thermophotovoltaic energy conversion for solar applications. Since then he has been actively involved in photovoltaics research. He is presently an Associate Professor of Electrical Engineering at Stanford University and heads a photovoltaics research team. This team has produced a new type of silicon solar cell with 28.3-percent efficiency. He has written over 50 published technical papers.

Dr. Swanson is a member of the American Physical Society, the Electrochemical Society, the AAAS, the International Solar Energy Society, Sigma Chi, Tau Beta Pi, and Eta Kappa Nu. He is presently a member of the Electronic Materials Committee of the AIME and the Power Generation Committee of the IEEE Power Engineering Society.